Fundamentals of Electrical Conductivity in Polymers

Xoan F. Sánchez-Romate

Abstract The fundamentals of electrical conductivity in polymers have been explored, more specifically, in conductive nanofilled-based polymers. First, the determination of the percolation threshold was investigated as it constitutes a crucial parameter to enable electrical networks throughout the polymer media. Furthermore, the electrical transport mechanisms of electrically conductive polymers were identified. Particularly, intrinsic conductivity of nanofiller, contact, and tunneling resistance was identified as the main transport mechanisms, being very affected by the nature of the insulating media as well as the geometry and interactions of the nanofillers. Furthermore, the electromechanical properties of conductive polymers have been also explored, where the tunneling transport mechanisms play a very prevalent role, leading to very high electrical sensitivities to mechanical strain. Temperature dependance of the electrical conductivity has been also investigated, and electro-thermal capabilities of electrically conductive polymers were determined, highlighting the high correlation between the electrical conductivity and the heating efficiency by Joule's effect. Finally, some interesting applications of electrically conductive polymers were discussed where the development of strain and damage sensors and electrothermal heaters for de-icing and self-healable systems were identified among the most interesting ones.

Keywords Electrical properties · Polymers · Percolation threshold · Nanocomposites · Joule's effect · Electromechanical properties

1 Introduction

Nowadays, there is an increasing interest in polymer science. The reason lies in the fact that polymers usually present many interesting properties such as inherent corrosion resistance, lightness, and a good balance of mechanical properties, especially

X. F. Sánchez-Romate (✉)
Materials Science and Engineering Area, Escuela Superior de Ciencias Experimentales Y Tecnología, University Rey Juan Carlos, C/Tulipán S/N, 28933 Mostoles, Spain
e-mail: xoan.fernandez.sanchezromate@urjc.es

N. Hameed et al. (eds.), *Multifunctional Epoxy Resins*, Engineering Materials,
https://doi.org/10.1007/978-981-19-6038-3_12

in thermosets. This combination of properties makes polymers very useful in a wide range of applications.

Among the different properties of polymers, the electrical ones are quite interesting. In this regard, polymers are insulating by nature. In fact, the measurement of their dielectric constant has been subject of a deep investigation since the first studies reported by Senturia and Shepperd in 1986 [1] where they investigated the dielectric analysis during thermosetting curing.

In general, the main transport mechanism in polymer matrices is the ionic conductivity, and the electrical properties are significantly influenced by the ionic mobility during the curing process, as it is affected by the time, temperature, and frequency of the measurements. Regarding to this, Johari [2] studied the effect of these parameters on the electrical conductivity of epoxy resins, correlating the changes in some physical features such as viscosity during curing with the diffusion coefficient or impurity ions, which affected the electrical properties of the resin.

It has been pointed out that the electrical properties of conventional polymers have been widely studied. However, their insulating nature limits their applications in multiple fields. In this context, in the last decades, there have been an extensively development of electrically conductive polymers, as they can open a wide range of novel functionalities over the traditional polymers. These conductive polymers are based on the addition of conductive nanofillers inside the insulating media to create electrical networks. The understanding of the main mechanisms of electrical conductivity of this type of polymers is, thus, crucial for a proper development of novel functionalities.

Therefore, this chapter will be focused on the electrical properties of electrically conductive polymers. First, the main electrical transport mechanisms will be discussed, by exploring the effect of the insulating media as well as the conductive nanofillers. In addition, theoretical models will be explored to better understand the correlations between the different parameters on the electrical properties of conductive polymers. Furthermore, the complex analysis under AC electric field will be also explored, as it will give further information about the role of the insulating media and the interactions with the conductive elements. The temperature dependance of the electrical conductivity will be also investigated, as it will have a significant effect on the main transport mechanisms in both the insulating media (as it will affect the ionic mobility) and the conductive one. Moreover, electro-thermal capabilities of electrically conductive polymers will be discussed, by correlating the electrical properties of conductive polymers with their resistive heating capabilities.

Finally, a summary of some interesting applications of electrically conductive polymers will be listed, from strain sensors for wearable and structural devices to electro-thermal heaters for de-icing and self-healing applications.

2 Electrical Transport of Electrically Conductive Resins

As commented before, conventional polymers are insulating by nature. This is a limitation for a great number of applications requiring a certain level of electrical conductivity.

In this regard, the addition of conductive nanoparticles is a solution to achieve electrically conductive resins. The principle is based on the fact that their inclusion induces the creation of electrical pathways inside the material. These electrical pathways, once above a certain threshold, promote the creation of a continuous electrical network, and thus, the electrical conductivity may increase several orders of magnitude, leading from an insulating to an electrically conductive material.

2.1 Conductive Fillers

Therefore, electrically conductive resins consist of a non-conductive polymer matrix and conductive fillers. The conductive fillers include metal fillers, carbon-based fillers, ceramic fillers, and metal-coated fillers [3]:

- *Metal fillers*: Metal fillers comprise metal particles with diameters below 20 μm. They can be classified into silver (Ag), gold (Au), nickel (Ni), and copper (Cu), and they are now widely used at nanoscale (that is, with average size of around 10^{-9} nm) due to their exceptional properties at this scale. Silver particles present unique electrical and thermal properties and are usually used in the form of flakes with loadings between 15 and 30 wt.%. [4]. Gold particles are commonly used in electronics due to their good electrical conductivity and corrosion and oxidation resistance. Nickel particles are usually used in a spherical form. They possess higher electrical resistivity than silver ones, although a good oxidation and corrosion resistance. Finally, copper particles present excellent electrical properties although the oxidation of the particles may be a problem.
- *Carbon-based fillers*: Carbon-based nanofillers are usually divided accordingly to their geometry into 0D, 1D, and 2D nanoparticles. 0D nanoparticles are those that do not present any characteristic dimension outside the nanometer scale. Here, carbon black and fullerenes are among the most used nanofillers. 1D nanoparticles are those that present one characteristic dimension outside the nanometer scale (the length) and the other two in the range of nanometers (the diameter). Single-walled or multi-walled carbon nanotubes (SWCNTs, MWCNTs) and carbon nanofibers (CNFs) are the most used. The first one presents superior mechanical and electrical properties, whereas the second ones are much more cost-efficient [5]. Finally, 2D nanoparticles are those that present two characteristic dimensions outside the nanoscale (diameter) and the other one at nanoscale level (thickness). Graphene and graphene nanoplatelets (GNPs) are the most common nanoparticles used as it present outstanding in-plane electrical and thermal conductivity.

- *Ceramic fillers*: Ceramic fillers usually present semiconductive characteristics. In this regard, BaFe, BN, TiB2, TiN, and SiC are among the most common fillers for polymer matrices. However, in most cases, due to their semiconductive characteristics, they are used as secondary fillers for enhancing electrical and thermal conductivity [6].
- *Metal-coated fillers*: Metal-coated fillers can be categorized into two wide types involving metal core and non-metal core particles. The non-metal core materials include carbon-based fillers, glass, or polymers coated with silver, gold, nickel, aluminum, or chromium. They promote an enhancement on the electrical conductivity but also on the resistance to oxidation or to moisture, which is a relevant problem in several resins, such as epoxy polymers.

Apart from metallic, carbon-based, ceramic or metal-coated fillers, there are also a wide investigation in the use of conductive polymers as fillers to enhance the electrical properties of resins. These conductive polymers are organic materials which possess electro-conductivity due to their unique structure. Here, polypyrrole (PPy) and polyaniline (PANI) are among the most extensively studied inherently conductive polymers.

Table 1 summarizes some of the most relevant results concerning electrical conductivity of different nanocomposites depending on the type of conductive filler.

Once described the most typical fillers used to enhance the electrical conductivity of polymer matrices, it is important to defined and explore a critical parameter; the percolation threshold, as it plays a dominant role in the electrical transport of nanoparticle-based polymers.

2.2 Percolation Threshold

The percolation threshold is defined as the critical volume fraction of nano or microparticles where the polymer system becomes electrically conductive, that is, where the electrical pathways are created throughout the material.

The determination of the percolation threshold is a key factor to understand the electrical properties of nanoparticle-based polymer systems. In this regard, there are a great number of parameters that affect the determination of the percolation threshold.

On the one hand, the geometry of the nanoparticles plays a very prevalent role. It is well known that the percolation threshold is inversely proportional to the aspect ratio of the nanoparticles, defined as the ratio between the maximum and the minimum characteristic dimensions. Therefore, the higher the aspect ratio of the nanoparticles is the lower the critical volume fraction needed to create the electrical pathways throughout the material.

Apart from the aspect ratio of the nanoparticles, the intrinsic 0D, 1D, or 2D nature of the nanoparticles also have a very dominant role in the determination of the percolation threshold. More specifically, it has been proved that 2D nanoparticles present values of percolation threshold significantly higher than 1D ones.

Table 1 Summary of maximum electrical conductivity and volume fraction needed for different nanofilled-based polymer composites (some data was extracted from [3])

Main filler	Additional filler	Treatment	Volume fraction (wt.%)	σ_{max} (S/m)	References
Silver nanoparticles	–	Silane-based coupling agent	5	3.99×10^{-2}	[7]
MWCNTs	–	Mixed curing agent-assisted layer-by-layer method	15	12	[8]
MWCNTs	–	Three-roll milling	0.3	0.1	[9]
SWCNT	–	Purified	0.005	2×10^{-2}	[10]
CNF	Magnetite nanoparticles	Coating by magnetite, weak magnetic field alignment	0.2	1×10^{-9}	
GNPs	–	Ultrasonication	8	1	[11]
Graphene	–	PSS (noncovalent functionalization)	1.2	1×10^{-2}	[12]
BaFe	PANI	–	–	6.1×10^{-4}	[13]
Graphene	Gold	Gold functionalization	1	1×10^{-4}	[14]
GO	Polypyrrole (PPy)	PPy coating	0.5	6.5×10^{-5}	[15]

For example, graphene-based nanocomposites usually present values of percolation threshold around 1 to 10 wt.% [16], whereas the percolation threshold of carbon nanotube-based nanocomposites is usually below 0.1 wt.% [9]. On the other hand, nanocomposites based in 0D particles such as fullerene and carbon black present values of percolation threshold usually above 10 wt.% due to their low aspect ratio in comparison with 1D and 2D nanoparticles [17]. The reason lies in the fact that 1D particles present a very high aspect ratio in comparison with 0D and 2D nanoparticles, and thus, it is easier to create efficient electrical pathways inside the material even at low nanofiller contents.

Another important parameter affecting the determination of the percolation threshold is the waviness of the nanoparticles. The waviness ratio is defined as the effective length of the nanoparticle (i.e., the nanotube) divided by its actual length, as shown in the schematics of Fig. 1. Here, the higher the waviness ratio is the higher the percolation threshold will be, as the effective aspect ratio is reduced, and thus, the electrical transport mechanisms are less efficient. In this context, some studies demonstrated that the percolation threshold of, for example, functionalized nanoparticles are quite above than the percolation threshold of non-functionalized ones [18].

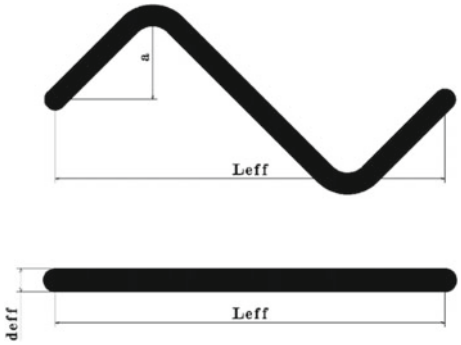

Fig. 1 Schematics of a CNT where the upper one denotes the real wavy CNT and the lower one the equivalent one. Here, the waviness ratio is defined as the amplitude, a, of the wavy CNT divided by L_{eff} (reproduced with permission from [18])

This is explained by their higher waviness ratio due to the lateral distortions induced by the functional groups [19].

The geometry of the nanofillers, thus, plays a very prevalent role. However, not only the geometry influences the percolation threshold, but also the dispersion state of the nanofillers, that is, their distribution within the polymer.

First, it is important to briefly describe the most common methods for dispersion of nanoparticles in polymer matrices. The aim of these methods is to achieve a homogeneous distribution of the nanoparticles as well as avoiding the presence of larger aggregates. In this regard, some methods are based in the prevalent action of shear forces to induce the disaggregation of larger agglomerates. More specifically, three-roll milling and toroidal stirring are among the most used dispersion techniques.

Three-roll milling consists in a progressive reduction of the gap between three rolls that are rotating at different speeds. Here, the higher the rotating speed or the lower the gap between adjacent rolls is the higher the shear forces induced in the mixture. Moreover, the resin also plays a very prevalent role as the shear forces involved are proportional to the viscosity of the mixture. Therefore, resins with higher viscosity will induce more prevalent shear forces during the dispersion process making it more efficient.

On the other hand, toroidal stirring consists in the induction of a toroidal 3D flow on the mixture that promotes a high homogenization of the nanoparticles as well as a good disaggregation of larger agglomerates. The principle for this disaggregation is the same than in case of three-roll milling, that is, the action of the shear forces induced by the blade. Here, the rotating speed of the blades, as well as the distance between the blades and the walls of the container, is the most important parameters that affect the effectiveness of the dispersion procedure. More specifically, the lower the gap between the blades and the walls or the higher the rotating speed is the higher the shear forces induced during the dispersion.

Apart from the dispersion procedures based on the action of shear forces, there are other techniques used to achieve a proper dispersion of the nanoparticles. For example, ultrasonication is one of the most common dispersion techniques for nanoparticles in low-viscosity resins. It is based on the emission of ultrasonic pulses that induces the breakage of larger agglomerates by the action of cavitation forces

in the fluid media. Here, the most important parameters of the dispersion procedure are the sonication time and the viscosity of the mixture. As expected, the increasing sonication time promotes a larger breakage of aggregates, whereas the viscosity acts in the opposite way as the higher the viscosity of the mixture, the lower the cavitation forces induced and thus, the lower the effectiveness of the ultrasonication process. In this regard, it is very common to use solvents during the dispersion process to reduce the viscosity of the mixture. These solvents are removed after the dispersion is achieved to avoid the formation of voids and generalized porosity in the final nanocomposite.

Therefore, once explained the most common techniques for the dispersion of nanoparticles in polymer systems, it is important to explore how the dispersion state affects the electrical properties of the final nanocomposite.

In this regard, there are several studies that investigate the correlations between the dispersion state and the electrical network created. More specifically, Li et al. [20] proposed a simple analytical model correlating some geometry factors and the dispersion state with the percolation threshold, P_c, of the system for CNT-doped nanocomposites:

$$P_c = \frac{\xi \varepsilon \pi}{6} + \frac{(1-\varepsilon)27\pi d^2}{4l^2} \tag{1}$$

where ξ is the proportion of the CNTs that are in form of aggregates, ε is the entanglement degree of the CNTs inside an agglomerate, and d and l are the average diameter and length of the CNTs, respectively.

Therefore, a high value of ξ would imply that most of CNTs are aggregated, that is, the dispersion state is not very good. On the other hand, a high value of ε would imply that the degree of entanglement of the CNTs inside the aggregates would be very high. A high value of aggregation parameters would lead, thus, to an increase of the percolation threshold, making the electrical network much less efficient.

As a general fact, therefore, it can be observed that the higher the aggregation of the nanoparticles is the higher the percolation threshold will be. This can be easily explained because well-dispersed nanoparticles promote the creation of more efficient electrical networks inside the material, as the distribution of these electrical pathways is much more homogeneous, as it can be observed in the schematics of Fig. 2.

Furthermore, by using this analytical model, it is possible to better understand the effect of the mentioned dispersion procedures on the percolation threshold by analyzing the dispersion achieved and the possible geometric modifications during the dispersion.

More specifically, it can be observed that ultrasonication is the most efficient technique in terms of disaggregation of larger aggregates, as the cavitation forces are, generally, very aggressive. However, it also induces a much more prevalent breakage of the nanoparticles themselves, leading to a reduction of their effective aspect ratio. In case of three-roll milling or mechanical stirring, the aggregation parameters are significantly higher, whereas the breakage of the nanoparticles is much less prevalent.

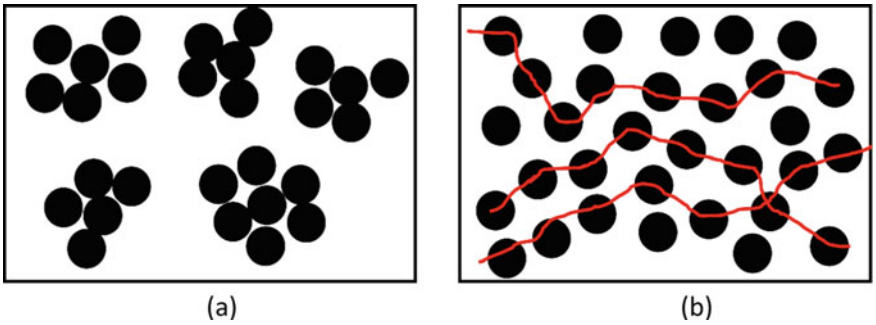

Fig. 2 Schematics of nanoparticle distribution for **a** an aggregated dispersion and **b** well-dispersed nanoparticles, where the red lines denote the main electrical pathways

2.3 Electrical Conductivity

Once understood how the electrical pathways are created and the importance of a proper determination of the percolation threshold; it is time to evaluate how these parameters affect the electrical properties of the nanocomposites. In this regard, the calculation of the electrical conductivity is a subject of huge interest.

2.3.1 Scaling Rule Model

As commented before, the percolation threshold is a critical parameter to determine the electrical properties of the final nanocomposites. Some analytical models for calculating the electrical conductivity are based in a scaling rule as follows:

$$\sigma_c = \sigma_0 \cdot (\phi - \phi_c)^t \tag{2}$$

where σ_0 is an invariable factor that depends on the aspect ratio of the nanoparticles, φ and φ_c are the volume fraction of the nanofiller and the percolation threshold, respectively, and t is an experimental fitting exponent which usually ranges from 1.3 to 2.

This model offers an initial evaluation of the electrical properties of the nanocomposite as a function of nanofiller content. However, it usually does not fit very well the experimental measurements, especially in nanofiller contents around the percolation threshold, where the changes in the electrical conductivity are very prevalent due to the changes in the main electrical transport mechanisms that occurs at these contents.

In these models, the percolation threshold is usually taken as a fixed parameter that is constant for each system. However, it significantly depends on the current dispersion state of the nanofillers inside the material. In fact, it has been proved that, during curing, the percolation threshold of the system changes, as the dispersion state

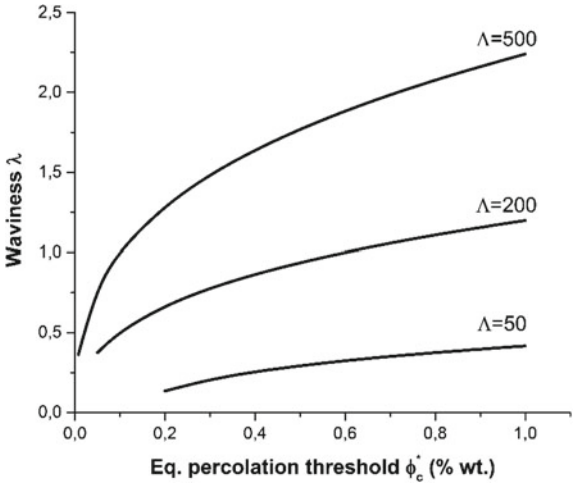

Fig. 3 Equivalent percolation threshold as a function of the waviness ratio, λ, and the aspect ratio, Λ, of the carbon nanofillers (reproduced with permission from [18])

of the nanofillers also changes because of a reaggregation before the gelation occurs [21].

Therefore, an equivalent percolation threshold was defined by Sánchez-Romate et al. [18]. This novel approach supposes that the percolation threshold is not a fixed parameter that depends on a fixed geometry and dispersion state, unique for each system, but a variable parameter that changes with the actual nanofiller content as it affects the interactions and distribution of the nanofillers. In other words, for a better understanding, this novel approach assumes that the percolation threshold depends on the actual dispersion state of the nanoparticles. It means that, for example, the percolation threshold increases with nanofiller content, as the aggregation of the nanoparticles is much more prevalent, and thus, the electrical pathways are much less efficient, accordingly to the model presented in Eq. (1).

This novel analytical method also takes geometry parameters such as the waviness or the aspect ratio of the nanoparticles, into account for the determination of the equivalent percolation threshold, as shown in the graph of Fig. 3. Here, it can be observed that the higher the waviness ratio of the nanofillers, the higher the percolation threshold, as the entanglement of the nanoparticles is much more prevalent, and thus, the electrical pathways created are less efficient.

Although the scaling law can offer an initial approximation, it does not really reflect the main electrical transport mechanisms governing nanofilled conductive polymers. In this regard, it is important to deeply explore these mechanisms to better understand the electrical properties of these systems.

2.3.2 Electrical Transport Mechanisms

In general, there are three main electrical transport mechanisms governing the nanofilled conductive polymers: the intrinsic electrical conductivity of the nanofillers,

the contact resistance between adjacent nanofillers, and the tunneling resistance between neighboring nanofillers that are not in direct contact.

The first mechanism only depends on the electrical properties of the nanofiller, and thus, it is out of scope of this chapter. However, the contact and the tunneling resistance between nanoparticles are very affected by the insulating media, that is, the polymer matrix, so it will be explored in the present throughout the chapter.

In this regard, it is important to define the tunneling effect. It is correlated with the probability of hoping conduction between two conductive particles that are separated by a thin insulating media. As a general fact, the higher the transmission probability, the lower the electrical resistance associated to this tunneling effect.

There are a lot of research exploring the tunneling effect in nanocomposites. More specifically, the electrical resistance associated to tunneling effect, R_{tunnel}, can be calculated from the following formula:

$$R_{\text{tunnel}} = \frac{h^2 t}{Ae^2\sqrt{2m\varphi}} exp\left(\frac{4\pi t}{h}\sqrt{2m\varphi}\right) \tag{3}$$

where m and e are the mass and charge of an electron, t *is* the interparticle distance, also called, tunneling distance, A is the cross-section area throughout the electron transmission may occur, also called tunneling area, and ϕ is the height barrier of the insulating media, which mainly depends on the nature of the polymer matrix.

Therefore, there are several parameters that govern the tunneling transport mechanism. More specifically, considering the mass and charge of the electron as invariable parameters, it is important to deeply study the effect of the others, that is, the tunneling distance, the tunneling area, and the height barrier of the polymer matrix.

Determination of Tunneling Distance

The tunneling distance, as mentioned earlier, is determined from the interparticle distance between adjacent and neighboring nanoparticles. Therefore, it heavily depends on the distribution of the nanoparticles inside the polymer media. Generally, the interparticle distance decreases by increasing the nanofiller content. More specifically, some studies propose a correlation between the interparticle distance and the volume fraction of the nanofillers as follows [22]:

$$t = t_c\left(\frac{\phi_c}{\phi}\right)^{\alpha} \tag{4}$$

where t and t_c are the tunneling distance at a determined volume fraction of nanoparticles, φ, and at percolation threshold, φ_c, defined as a fixed interparticle distance of 1.4 nm, respectively, and α is an experimental exponent which depends on the maximum compaction of the nanofillers.

Therefore, by increasing the volume fraction of the nanofiller, the tunneling distance between neighboring nanoparticles will be decrease, and thus, the electrical resistance associated to tunneling resistance will be also decreased.

However, the expression set in Eq. (4) is quite simple and does not take aggregation parameters into account. In this regard, there are several models that also study the influence of the nanofiller aggregation in the tunneling distance between nanoparticles. It can be considered that the interparticle distance inside an aggregate is the minimum distance between nanoparticles, set as 0.34 nm for nanofillers that are in direct contact. Outside the aggregates, the interparticle distance is significantly higher. Therefore, the mean interparticle distance does not only depend on the volume fraction of the nanofiller but also on the dispersion state.

Effect of Tunneling Area

The determination of the tunneling area throughout the tunneling transport may occur is also a very crucial factor to determine the electrical properties of the nanocomposites. This tunneling area mainly depends on the geometry of the nanofillers and the type of contact between adjacent and neighboring nanoparticles.

In this regard, several studies have explored the influence of the tunneling area and type of contact in the electrical properties of nanocomposites. For example, Kuronuma et al. [23] proposed an analytical model for the determination of tunneling resistance in CNT-doped polymers. They supposed that the contact between nanotubes may occur in-plane or out-of-plane. In the first case, the tunneling area, A_I, can be estimated as follows:

$$A_I = \frac{\pi d^2}{4} \tag{5}$$

where d is the outer diameter of the nanotube.

In case of out-of-plane contacts, the tunneling area, A_{II}, can be estimated by using the following formula:

$$A_{II} = d^2 \tag{6}$$

In both cases, the differences between the tunneling area for in-plane and out-of-plane contacts are quite slight. However, in case of 2D nanoparticles, the differences may be much more prevalent.

In this context, some studies have proposed different approximations of the tunneling area for [24] in-plane and out-of-plane contact in case of 2D nanoparticles, as observed in the schematics of Fig. 4. Here, the tunneling area for in-plane contacts may be estimated as follows:

$$A_{II} = l \cdot t \tag{7}$$

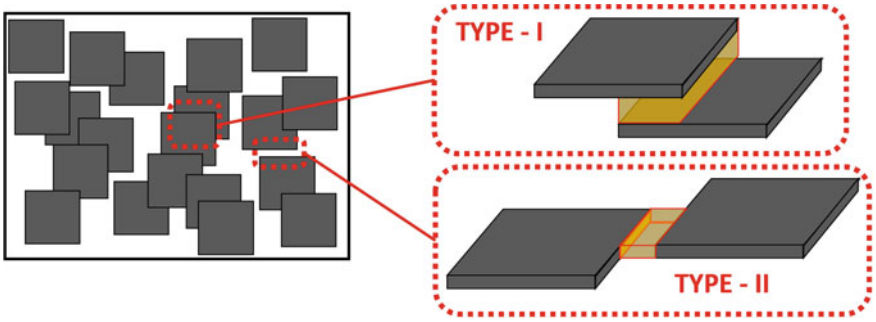

Fig. 4 Schematics of in-plane and out-of-plane contacts in a GNP network (reproduced with permission from [24])

where l and t are the average length (diameter) and the average thickness of the nanoplatelet, respectively.

However, in case of out-of-plane contacts, the estimation is quite more complicated than for nanotubes. A first simple approximation may suppose the tunneling area as a mean value of the total diameter of the nanoplatelet, by using the following expression:

$$A_I = \frac{l^2}{2} \tag{8}$$

Therefore, since $l \gg t$, the out-of-plane and in-plane tunneling areas are significantly different. For this reason, thus, the prevalence of in-plane or out-of-plane mechanisms will play a relevant role in the estimation of the electrical properties of the nanocomposite.

Effect of the Height Barrier

The height barrier of the polymer matrix, as commented, is the other parameter that plays an important role on the electrical transport mechanisms in nanocomposites, especially, at lower nanofiller loadings, since the tunneling mechanisms are most predominant in these cases. For example, the typical values of height barrier for epoxy resins usually range from 0.5 to 2.5 eV [25]. Therefore, depending on the estimated value of the height barrier, the electrical conductivity will change. More specifically, as observed in the graphs of Fig. 5, the electrical conductivity decreases with increasing height barrier from 0.5 to 2.5 eV in several orders of magnitude, accordingly to the expression of Eq. (3). These differences in the electrical conductivity are more prevalent at lower nanofiller contents, as commented before, due to a much more prevalent role of the insulating media in the electrical transport properties of the nanocomposite.

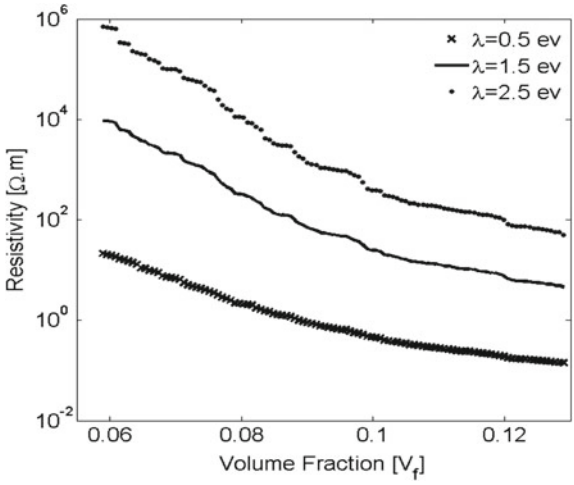

Fig. 5 Electrical resistivity as a function of height barrier of an epoxy matrix and volume fraction of the nanofiller (reproduced from [25] under Creative Commons CC-BY license)

2.3.3 Analytical Models for Electrical Conductivity Estimation

Therefore, once estimated the main transport mechanisms and how they are affected by the geometry, dispersion state and type of contact of the nanofillers, as well as by the height barrier of the insulating media, it is time to explore how it is reflected in, for example, the determination the electrical conductivity of polymer nanocomposites.

In this regard, Sánchez-Romate et al. [9] proposed a very simple analytical model for the calculation of the electrical conductivity of nanofilled polymer matrices that is reflected in the schematics of Fig. 6. It is based on a block model which assumes that the material may be divided in three main regions: one, which is dominated by the larger aggregates, where the main conduction mechanisms are governed by the intrinsic electrical conductivity of the nanofillers and the contact resistance between adjacent nanoparticles. The second region, also called the well-dispersed area, is given by these regions where the nanoparticles are not in contact but the interparticle distance is low enough to guarantee the conduction mechanisms by tunneling effect. Therefore, here, the main transport mechanism is given by the tunneling resistance. Finally, the third region, also called non-percolated area, is given by the zones of the material where there are not enough nanoparticles to guarantee a proper electrical network and thus, can be considered as an insulating region.

By dividing the material in these three main blocks, the electrical conductivity can be estimated as follows:

$$\frac{1}{R} = \xi_a \cdot \frac{1}{R_a} + \xi_d \cdot \frac{1}{R_d} + \underbrace{\xi_{non} \cdot \frac{1}{R_\infty}}_{\sim 0} \rightarrow R = \frac{R_a R_d}{(\xi_d R_a + \xi_a R_d)} \tag{9}$$

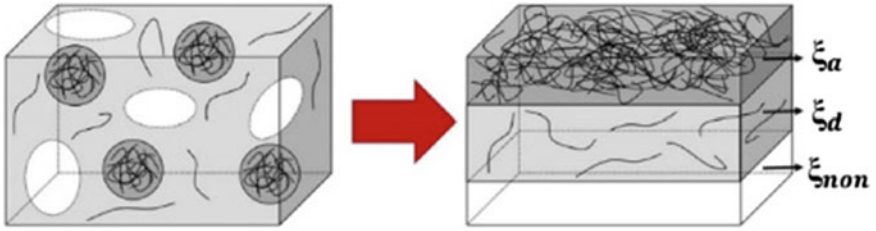

Fig. 6 Schematic of the proposed model in [9] showing (left) the real dispersion state and (right) the equivalent block disposition (reproduced with permission from [9])

where R is the equivalent electrical resistance of the element, and ξ_a, ξ_d, and ξ_{non} are the volume fractions of the agglomerated, well-dispersed, and non-percolated regions.

Therefore, by using this simple analytical model, it is possible to determine the correlation between the dispersion state and the electrical conductivity of the nanocomposite by taking the transport phenomena previously described. In this context, an aggregation parameter is defined as the ratio between the fraction of aggregated areas and the well-dispersed ones; $\varphi = \xi_a/\xi_d$.

Here, it can be observed that the electrical conductivity decreases by increasing the aggregation ratio. This is explained because the presence of larger agglomerates affects the creation of efficient electrical networks, as previously described. More specifically, by increasing the fraction of aggregated areas, also increases the fraction of non-percolated regions as the nanoparticles are much more entangled and thus occupy a lower volume fraction. As the correlation between the interparticle distance and the tunneling resistance follows a linear-exponential law, this would explain the lower efficiency of the electrical networks in this case.

Another important parameter that must be considered also in the estimation of the electrical conductivity of nanomposites is the orientation of the nanofillers. There are many of studies exploring the influence of this parameter in the creation of the electrical networks inside the material [26, 27]. It was found that electrical conductivity increases with CNT alignment due to the creation of more percolating networks [28]. Therefore, the possible alignment of the nanofillers, especially in case of 1D nanoparticles, is also an important factor to consider in order to determine the electrical properties of the nanocomposite.

2.4 Electromechanical Properties

The electrical conductivity does not only depend on the dispersion state, polymer nature or nanofiller type, but also is conditioned by the mechanical constraints of the material.

More specifically, the electrical properties of nanofilled resins change with mechanical strain. The reason lies in the fact that, the application of an external strain field promotes the deformation of the electrical network, leading to changes in the interparticle distance and/or in the type of contact between adjacent nanoparticles.

Moreover, most of nanofillers are piezoresistive. It means that their electrical conductivity changes with the applied strain. Therefore, even the intrinsic electrical resistance of the conductive nanofillers may vary with the application of an external strain field.

In this regard, it can be assumed, that at low strain levels, the deformation of the nanofillers can be negligible, as the Young's modulus of the nanofillers is usually several orders of magnitude above the Young's modulus of the polymer matrix. Therefore, the variations of the electrical conductivity due to the piezoresistive response of the nanofillers can be neglected and, for this reason, the changes in the electrical conductivity when applying a strain field will be due to the changes in the electrical resistance by tunneling effect, as the interparticle distance changes.

Concerning Eq. (3), it can be elucidated that the tunneling resistance increases in a linear-exponential fashion with applied strain as the correlation between the tunneling distance, and the applied strain can be approximated by the following expression:

$$t = t_0 \cdot (1 + \varepsilon) \tag{10}$$

where t_0 denotes the initial tunneling distance at zero strain conditions.

Regarding the electromechanical properties, it is important to study a key parameter, the gauge factor. It is defined as the ratio between the change of the normalized resistance $\Delta R/R_0$ and the applied strain, ε. The gauge factor denotes the electrical sensitivity of the system under an applied strain. Therefore, the higher the gauge factor is the higher the sensitivity of the system will be.

In this context, as it can be observed in the graph of Fig. 7, the changes of the normalized resistance are more prevalent when increasing the tunneling distance, due to the linear-exponential correlation between the tunneling distance and the tunneling resistance. Therefore, it implies that the lower the nanofiller content, the higher the gauge factor that can be achieved as the interparticle distance will increase. More specifically, the nearer the nanofiller content to the percolation threshold of the system is the more electromechanical sensitive the system will be.

As commented before, the electromechanical response is also affected by the dispersion state of the nanofillers, their geometry and the type of contacts between adjacent and neighboring nanoparticles.

More specifically, the dispersion state has been found to be a critical factor that governs the electromechanical properties of nanocomposites. Furthermore, as explored in [9], the fraction of aggregated, well-dispersed, and non-percolated areas plays a dominant role in the gauge factor of the system.

As a general fact, the gauge factor was supposed to be higher near the percolation threshold, due to a higher interparticle distance. However, this statement is only true if the nanoparticles are homogenously dispersed within the polymer matrix. More

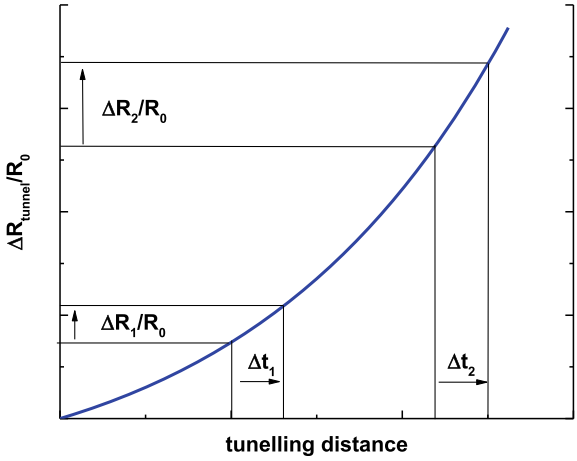

Fig. 7 Variation of the electrical resistance as a function of tunneling distance by using the expression from Eq. (3), where a linear-exponential correlation is observed

specifically, even a low nanofiller contents, if the aggregation ratio is very high, this will imply that the most prevalent conductive pathways take place throughout the aggregates. As commented before, the main conduction mechanisms inside larger aggregates are the intrinsic conductivity of the nanofiller itself. Therefore, the change of the electrical resistance with applied strain will not be as high as throughout the well-dispersed areas, where the interparticle distance is considerably higher.

On the opposite side, if the aggregation ratio is very low, this will imply that the most prevalent conduction mechanisms take place in the well-dispersed areas, that is, they will be governed by the tunneling effect. Therefore, the gauge factor will be increased.

In this regard, Fig. 8 shows the value of the gauge factor estimated by the model in [9] as a function of the mean interparticle distance and the aggregation ratio. It can be observed that the higher the aggregation ratio is the lower the value of interparticle distance where the maximum gauge factor is achieved. This can be explained because, at a very high fraction of aggregates, the main electrical mechanisms take place through the aggregates. It means that, if the interparticle distance in the well-dispersed regions is very high, these well-dispersed areas will not participate in the most prevalent electrical transport mechanisms, as the electrical resistance of these regions will be much higher than the electrical resistance of the aggregates. The opposite effect happens with a very low aggregation ratio, where the most prevalent electrical transport mechanisms take place through the well-dispersed regions, and thus, the gauge factor increases with interparticle distance.

Apart from the dispersion state, the type of contact between neighboring nanoparticles also plays a very prevalent role. Here, as commented before, in case of 1D nanoparticles such as nanotubes or nanowires, the slight differences between the tunneling area in in-plane and out-of-plane contacts are reflected in slight variations of the electromechanical behavior. However, in case of 2D nanoparticles, the

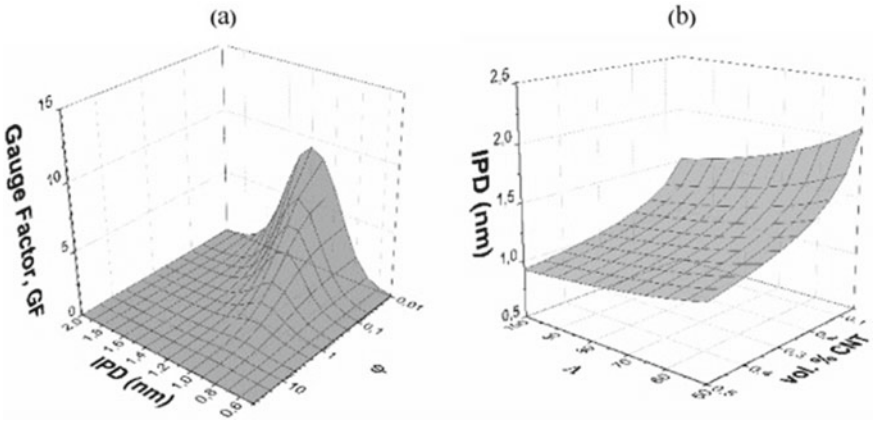

Fig. 8 **a** Effect of the aggregate ratio and interparticle distance (IPD) on the gauge factor (GF) and **b** effect of the aspect ratio and CNT content on the mean IPD (reproduced with permission from [9])

prevalence of in-plane or out-of-plane mechanisms will play a dominant role in the electromechanical response of the material.

In this context, Fig. 9 shows the electromechanical response under tensile conditions as a function of the fraction of in-plane and out-of-plane mechanisms. It can be observed that, by increasing the fraction of in-plane contacts, the sensitivity increases, whereas at very low fractions of in-plane mechanisms (under 0.1), the gauge factor is very low, even negative, due to the prevalence of Poisson effect.

Furthermore, the electromechanical response under compressive strain is quite more difficult to understand. Here, there are many mechanisms that take part. On the one side, the effect of the compressive strain itself that promotes a reduction in the interparticle distance between neighboring nanoparticles. On the other hand, the presence of local buckling mechanisms that may be reflected in the creation of microcavities [29], acting as disruptions in the electrical network.

The in-plane/out-of-plane models have been proved to be also an effective way to understand the electromechanical behavior under compressive strain. In fact, Fig. 10a summarizes the effect of in-plane/out-of-plane contact proportion on the electromechanical behavior of a GNP-epoxy nanocomposite under compressive strain. Here, it can be elucidated that the higher the in-plane proportion is the higher the electrical resistance decrease with applied strain will be. In this regard, this model has been proved to fit very well the experimental results obtained for compressive tests in GNP-epoxy nanocomposites (Fig. 10b). It can be observed that, at low strain levels, the electrical resistance decreases due to the decrease in the tunneling distance of in-plane contacts. However, at high strain levels, an increase of the electrical resistance is observed. This is explained by the presence of local buckling mechanisms as well as due to the prevalence of out-of-plane contacts, acting in an opposite way because of the Poisson effect. Therefore, as a general fact, the in-plane mechanisms dominate

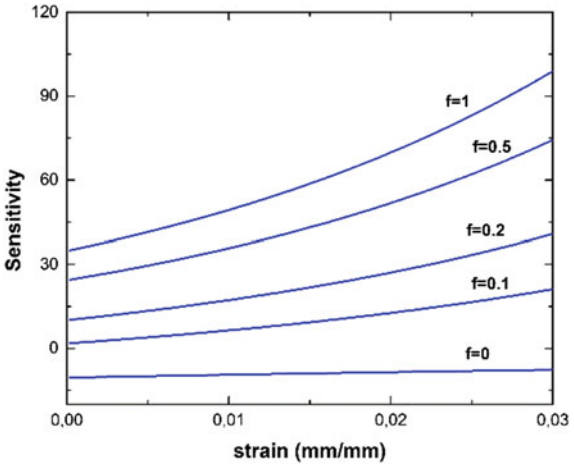

Fig. 9 Sensitivity estimated from the in-plane/out-of-plane contact model in [24] as a function of the applied strain, where f denotes the fraction of in-plane contacts in the network ($f = 1$ denotes a 100% proportion of in-plane contacts, whereas $f = 0$ denotes a 100% proportion of out-of-plane contacts) (reproduced with permission from [24])

the electromechanical response at low strains, whereas the out-of-plane mechanisms rule the electromechanical response at high strains.

The 1D or 2D nature of the nanoparticles also plays a prevalent role in the electromechanical capabilities of the nanocomposites. It can be observed that 2D nanoparticle-based composites usually present much higher gauge factor values than 1D nanoparticle-based ones. This can be easily explained accordingly to the expression in Eq. (3) by using the tunneling areas estimated from Eqs. (5–8). In case of 2D nanoparticles, the tunneling areas in both in-plane and out-of-plane contacts are generally much higher than in 1D nanoparticles, as $l \cdot t \gg d^2$. Therefore, the maximum interparticle distance between neighboring nanoparticles can be increased for 2D nanoparticles, and thus, the sensitivity increases due to the linear-exponential dependency with the tunneling distance. In fact, several studies have reported gauge factors of around 1–10 for nanotubes [31, 32], whereas it can be above 10–50 in case of nanoplatelets at low strain levels [16, 33].

Furthermore, the electromechanical response of 2D nanoparticle-based composites is usually much more exponential than in case of 1D nanoparticle-based ones, for the same reasons that those described before. In addition, the electromechanical response of hybrid 1D–2D nanoparticle-based composites has been also studied [34], to better understand the possible interactions in a hybrid network. Here, it can be noticed that the higher the ratio 2D to 1D nanoparticles is the higher the exponential behavior of the electrical response as a function of the applied strain will be, (Figs. 11a and b) as the number of electrical pathways through the 2D nanoparticle networks is increased, as observed in the schematics of Fig. 11c. Therefore, the

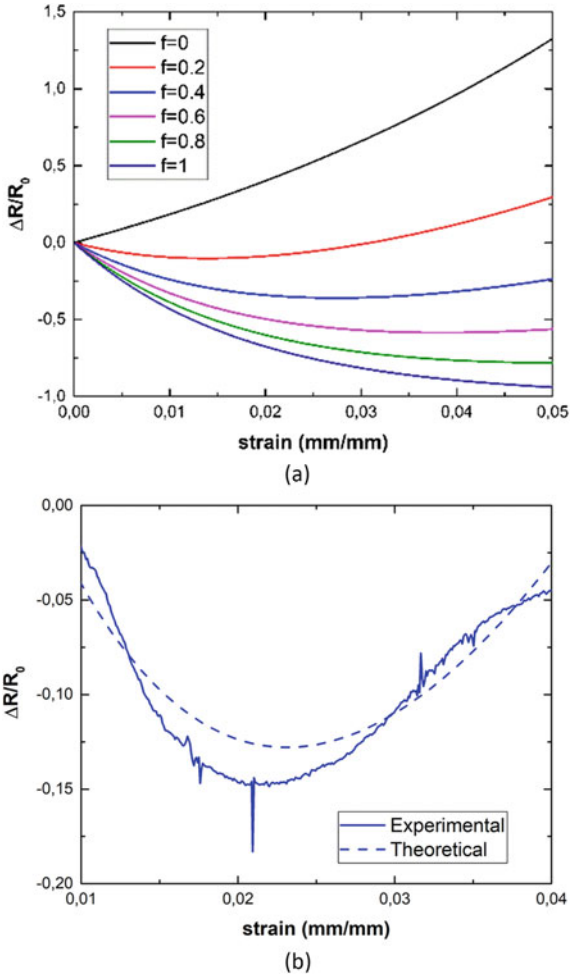

Fig. 10 Electromechanical behavior under compressive conditions showing **a** the influence of the f parameter (that is, the fraction of in-plane contacts) and **b** the theoretical to experimental comparison for a GNP-epoxy compressive test (reproduced with permission from [30])

selection of the type of nanoparticle is a very crucial factor for the development of electromechanical sensitive materials.

2.5 AC Electrical Analysis

Apart from the DC electrical conductivity, the nanocomposites also show complex, frequency-dependent electrical properties. In this regard, there are some investigations dealing with alternating current (AC) properties of nanofilled polymer matrices.

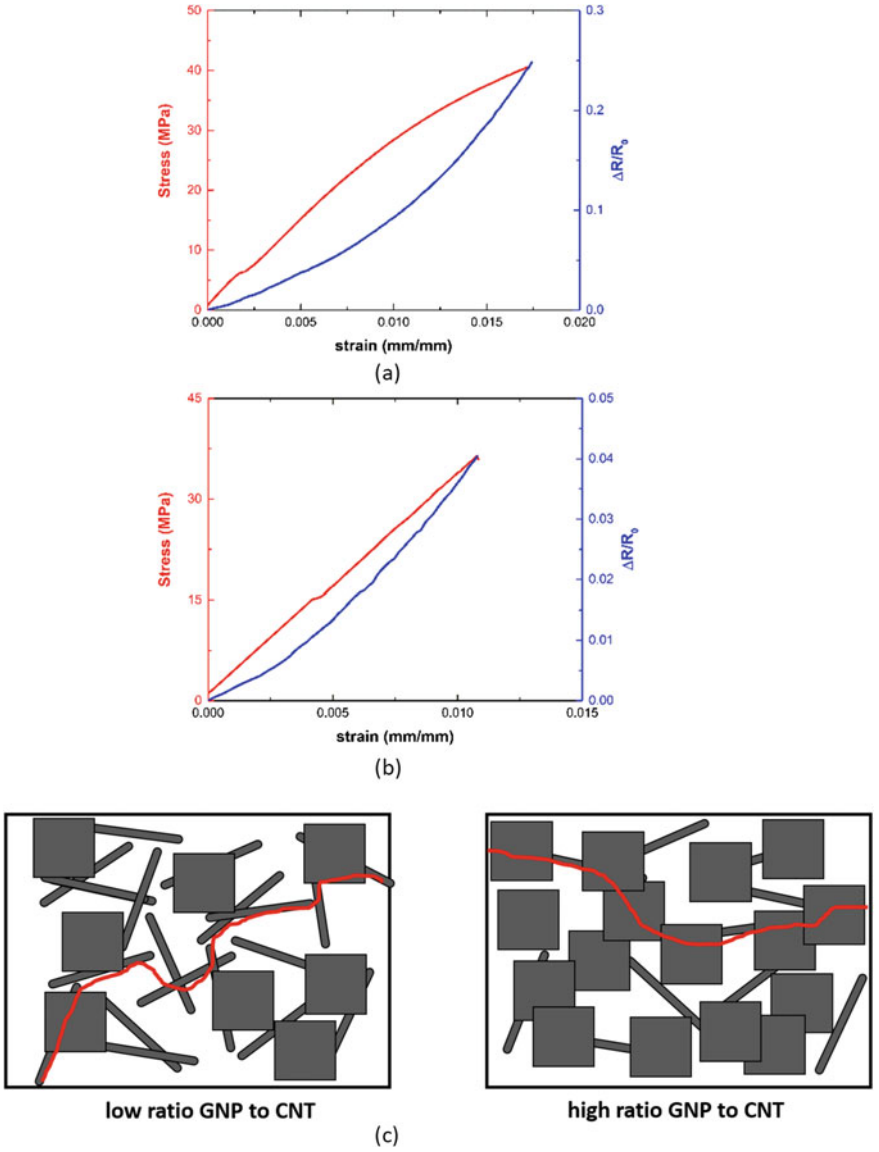

Fig. 11 Electromechanical behavior of **a** 5 wt.% GNP–0.2 wt.% CNT, **b** 5 wt.% GNP-0.1 wt.% CNT, and **c** schematics of electrical transport in a hybrid GNP-CNT network where the red line denotes the preferential electrical pathways (reproduced from [34] under Creative Commons CC-BY license)

As a general fact, the knowledge of the AC properties would allow to better understand the possible interactions among nanofillers and the particular effect of the insulating media on the electrical properties of the nanocomposites.

Figure 12 shows the typical Niqvist plot of the complex impedance as a function of AC frequency for an epoxy/CNF system. Here, it can be observed that both the real and imaginary parts of the complex impedance increase with decreasing the nanofiller content, in a similar way than in case of DC conductivity. More specifically, the electrical network can be modeled by a series–parallel circuit composed by an RC element, which corresponds to the tunneling effect occurring between adjacent nanoparticles and an LRC element, corresponding to the intrinsic and contact resistance between nanoparticles, as observed in the schematics of Fig. 13. Therefore, by adjusting the RC and LRC parameters, it is possible to quantify the effect of the intrinsic, contact, and tunneling mechanisms in the electrical properties of the nanocomposite. For example, a high RC/LRC ratio will be reflected in a high prevalence of the tunneling mechanisms inside the electrical network, typically for nanocomposites filled with low nanoparticle contents. However, a low RC/LRC ratio would denote a high prevalence of intrinsic and contact transport mechanisms, typically for nanocomposites filled with high nanoparticle contents.

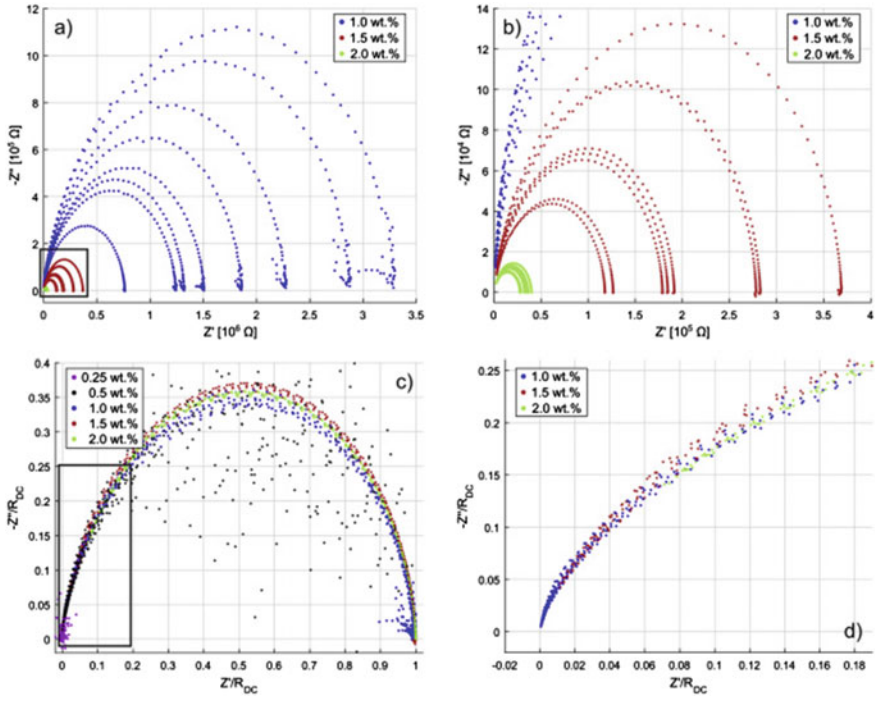

Fig. 12 **a** EIS data for 1.0, 1.5, and 2.0 wt% CNFs, **b** close up of boxed region from **a** showing 1.5 and 2.0 wt% more clearly, **c** EIS data for all weight fractions normalized by DC resistance, R_{DC}, and **d** close up of boxed region from **c** (reproduced with permission from [35])

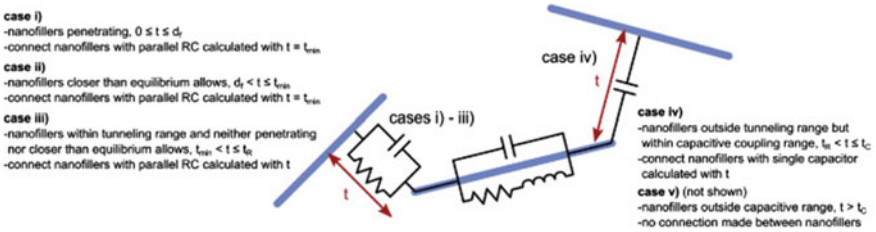

Fig. 13 Schematic of nanofiller and nanofiller-to-nanofiller junction. For cases **i–iii**, CNFs are proximate enough to enable inter-nanofiller electron tunneling. For case **iv**, it is assumed that the CNFs are too distant to participate in electron tunneling but near enough to enable inter-nanofiller capacitive coupling. Lastly, the intrinsic AC properties of the CNFs are modeled as a capacitor in parallel with a series resistor-inductor combination (reproduced with permission from [35])

The capacitance terms associated to tunneling effect can be explained by the formation of micro-capacitors between nanofillers due to the presence of a thin insulating layer between the conductive nanoparticles and can be modeled as follows:

$$C_j = \frac{\alpha \varepsilon_0 \varepsilon_r}{t} \tag{11}$$

where α is a scaling factor, ε_0 and ε_r are the permittivity of free space and the relative permittivity of epoxy, respectively, A *is* the overlapping area between nanofillers, which can be considered as the tunneling area, and t is the length of the thin layer, which can be considered as the tunneling distance.

On the other hand, the capacitance and inductance terms of the nanofillers, C_f and L_f, can be estimated from the following formulas:

$$C_f = \delta l C_q; \quad L_f = \zeta l L_k \tag{12}$$

where δ and ζ are two scaling factors, l is the length of the nanofiller; and C_q and L_k are the typical capacitance and inductance terms of the nanofillers that may be determined from the literature. For example, in case of CNTs, they have been estimated as $C_q = 100$ aF/μm and $L_k = 10$ nH/μm [36].

In addition, the effect of an applied strain on the complex impedance analysis is shown in the graphs of Fig. 14 for a GNP-PDMS system. Here, it can be observed that, at large deformations, there is an increase of both the real and the imaginary parts of the complex impedance. This is explained by the effect of out-of-plane contacts that, as explained before, play a relevant role at very high strains. As out-of-plane contacts promote an increase of the electrical resistance due to tunneling effect due to the separation of the nanofillers, it will be reflected in an increase of the capacitance term corresponding to the insulating media.

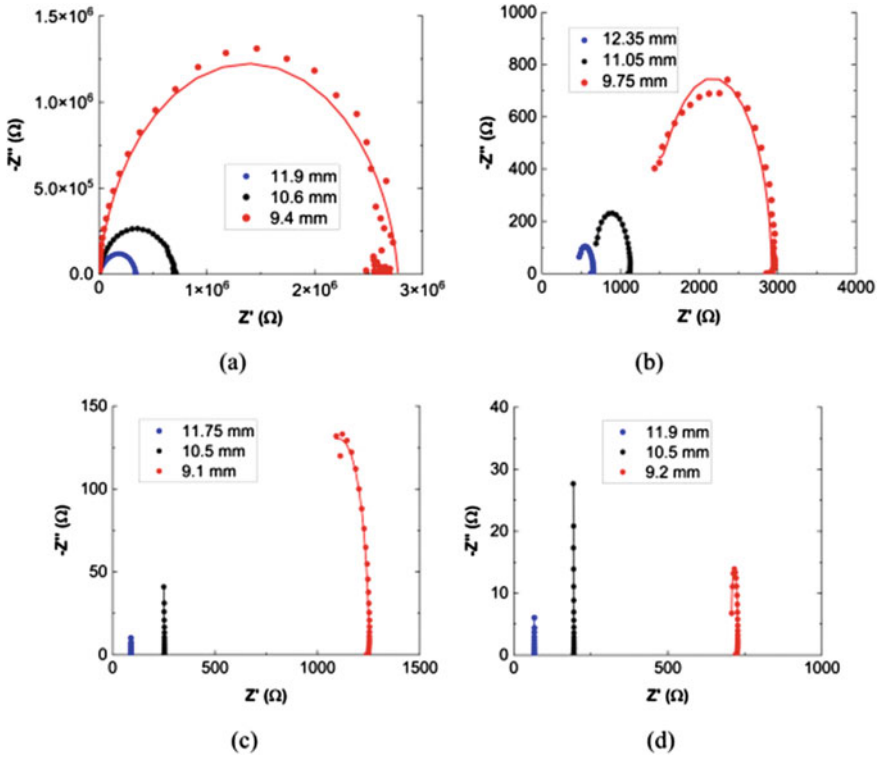

Fig. 14 EIS curves as a function of the compressive deformation for **a** 4, **b**, 6, **c** 8, and **d** 10 wt% GNP samples where the dots denote the experimental measurements and the solid lines the fitted data using the equivalent circuit (reproduced with permission from [37])

2.6 Temperature Dependance of Electrical Conductivity

The electrical conductivity does not only depend on the type and distribution of nanofillers inside the polymer matrix, but also on other factors such as the temperature. In fact, the effect of the temperature on the electrical conductivity of nanofilled polymers is quite complex to understand.

More specifically, the electrical properties as a function of the temperature highly depend on the nanofiller concentration. As explained before, for nanofiller contents below the percolation threshold, the insulating media dominates the electrical properties of the whole material as not enough electrical pathways are formed. On the other hand, for nanofiller contents above, the percolation threshold, the intrinsic, contact, and tunneling transport between adjacent and neighboring nanoparticles are the most dominating mechanisms governing the electrical properties of the nanocomposites.

Therefore, the temperature dependency of the electrical conductivity will be different depending on the nanofiller content, that is, if it is below or above percolation threshold.

In particular, the temperature effect on the tunneling conductivity can be approximated by the following formula [38]:

$$\sigma \sim \exp\left(-\frac{T_1}{T+T_0}\right) \tag{13}$$

Being

$$T_1 = \frac{wA\varepsilon_0^2}{8\pi k_B}; \quad T_0 = \frac{2T_1}{\pi \chi w} \tag{14}$$

where $\chi = \sqrt{\frac{2mV_0}{h^2}}$ and $\varepsilon_0 = \frac{4V_0}{ew}$, with e and m being the electron charge and mass, respectively, V_0 is the potential barrier height, w *is* the gap width, k_B is the Boltzmann constant, and A is the area of the nanoparticles.

Apart from the tunneling effect, which dominates when the nanofiller content is above the percolation threshold, there are other electrical transport mechanisms that governs the electrical properties of the polymer matrix.

On the one hand, the polymer matrix can be approximated filled with granular conductive materials, with a nanometer size, dispersed in the dielectric matrix. These granules can be formed by incomplete chemical reactions or by thermal variations during the curing process, resulting in trapped ions [39]. In this case, the electrical conductivity as a function of temperature can be estimated by applying the following expression:

$$\sigma \sim \sigma_0 + \ln\left[\frac{gE_c}{\max(T,\Gamma)}\right] + \sqrt{\frac{k_B T}{\Gamma}} \tag{15}$$

where σ_0 is related to the diffusion of the electrons from grain to grain, g is the dimensionless conductance ($g \gg 1$ in the strong coupling regime), E_c is the single-grain Coulomb charging energy, and Γ is a characteristic energy related to the tunneling conductance and the mean energy-level spacing.

Finally, the ionic conductivity is a very relevant electrical transport mechanisms inside the polymer matrix when below the grass transition temperature and is correlated to the presence of small concentrations of impurity molecules [40]. It can be given by the following formula:

$$\sigma \sim \sum_i \frac{A_i}{T} \exp\left(\frac{-Ea_i}{k_B T}\right) \tag{16}$$

where the sum runs for the different ionic species present in the system, Ea_i is the activation energy for a specific ionic species, and A_i is a constant associated with the electronic charge and the separation between neighboring potential walls for a characteristic ionic species.

Therefore, the electrical conductivity as a function of temperature can be calculated by taking all these effects into account, leading to the following formulas depending on the nanofiller content, that is, if the nanofiller content is below or above the percolation threshold:

$$\sigma \sim \sum_i \frac{A_i}{T}\exp\left(\frac{-Ea_i}{k_B T}\right) + \ln\left[\frac{gE_c}{\max(T,\Gamma)}\right] + \sqrt{\frac{k_B T}{\Gamma}} \quad \text{for } \phi < \phi_c \tag{17}$$

$$\sigma \sim \exp\left(-\frac{T_1}{T+T_0}\right) + \sum_i \frac{A_i}{T}\exp\left(\frac{-Ea_i}{k_B T}\right) + \ln\left[\frac{gE_c}{\max(T,\Gamma)}\right] + \sqrt{\frac{k_B T}{\Gamma}} \quad \text{for } \phi > \phi_c$$

These expressions, thus, allow to better understand the effect of the temperature on the electrical conductivity of a nanofilled polymer matrix. As a general fact, the ionic conductivity will increase with increasing the temperature and thus, at contents below the percolation threshold, the electrical conductivity will increase with temperature, as it is the main electrical transport mechanism.

However, at nanofiller contents above percolation threshold, tunneling transport mechanisms will play a very prevalent role in the electrical properties. Here, it is important to point out that, at nanofiller contents slightly above percolation threshold, tunneling resistance will be the most relevant electrical transport mechanism, whereas at nanofiller contents significantly above percolation threshold, the contact resistance will be the governing transport mechanism [41]. The tunneling resistance is reduced with temperature increase [42] as it depends on thermal fluctuations. However, the contact resistance has an opposite behavior with temperature since an increase in the temperature will enhance the kinetic energy of the carriers, and thus, contact resistance will increase due to scattering effects. For these reasons, the electrical conductivity of highly filled polymer composites usually decreases with temperature, as contact resistance is the most relevant transport mechanism. The effect of the temperature on the electrical conductivity as a function of nanofiller content is also described in the graph of Fig. 15.

2.7 Electro-Thermal Properties

The presence of electrically conductive nanofillers can offer a wide range of novel properties to the polymer matrix, as commented before. Here, the capability of heating by Joule's effect is one of the most interesting.

Joule's heating effect refers to the temperature increase in a conductive material due to the current flowing throughout it. More specifically, electrically conductive polymer matrices based on the addition of conductive nanofillers are susceptible to temperature increase when an electric field is applied. At atomic level, Joule's heating

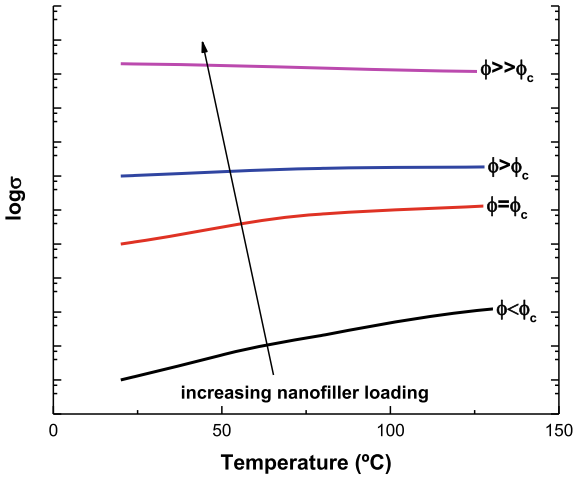

Fig. 15 Temperature dependance of the electrical conductivity of a nanofilled resin a function of the nanofiller loading showing the three typical behaviors: below percolation threshold; around or slightly above the percolation threshold and highly above the percolation threshold of the system

is a result of the movement of electrons that collides with atoms in a conductor. Therefore, impulses are transferred to the atoms, increasing their kinetic energy in form of heating.

As a general fact, the heating originated due to the applied voltage can be estimated by the well-known Joule's formula:

$$Q = I^2 Rt \tag{18}$$

where Q is the heating flow, I and R are the current flow and the electrical resistance of the material, respectively, and t is the time the electrical field is applied.

Therefore, there is a direct correlation between the Joule's heating capabilities and the electrical conductivity of the nanocomposites. Here, the presence of local aggregates of nanoparticles, defects, disruptions of the electrical network, etc., thus, will have a very significant impact on the Joule's heating capabilities of the material.

There are three main regimes when analyzing the heating by Joule's effect: the heating regime, which occurs in the first stages when applying the electric field; the maximum temperature regime, which occurs when the temperature is stabilized; and the cooling regime, which takes places once the electric field is not longer applied. The temperature can be estimated for each region by following these expressions [43, 44]:

$$\text{Heating regime} : T_t = (T_{\max} - T_0)\left(1 - e^{-\frac{t}{\tau_h}}\right) + T_0 \tag{19}$$

$$\text{Maximum temperature regime} : h_{r+c} = \frac{I_c V_0}{T_m - T_0} \tag{20}$$

$$\text{Cooling regime} : T_t = (T_{\max} - T_0)\left(e^{-\frac{t}{\tau_c}}\right) + T_0 \tag{21}$$

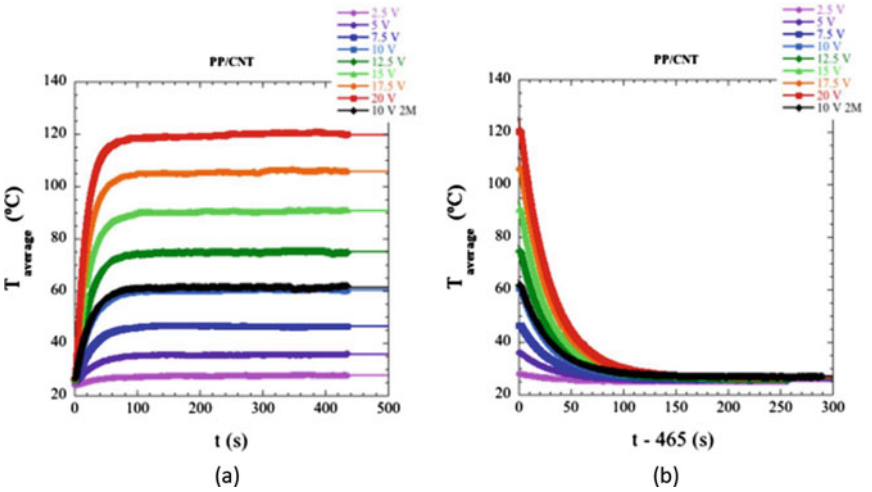

Fig. 16 **a** Heating and **b** cooling curves of PP/CNT nanocomposites as a function of applied voltage where the solid lines denote the theoretical fitting using expressions from Eqs. (19–21) (reproduced from [45] under creative commons CC-BY license)

where t is the time, $T_{\max}$ is the maximum temperature that can be reached, T_0 is the initial temperature, T_t is the temperature at each time or transient temperature, τ_h and τ_c are characteristic times, during heating and cooling, respectively, h_{r+c} is the heat transferred by radiation and convection, and I_c and V_0 are the current and applied voltage, respectively. A typical heating–cooling cycle is showed in the graphs of Fig. 16.

There are a lot of studies dealing with Joule's heating capabilities of nanofilled polymer composites for a multiple range of applications. Here, it is very common to plot the maximum temperature reached as a function of applied voltage. Usually, the correlation between the maximum temperature reached and the applied voltage follows a square law, due to the dependance between the heating flow and the current passing through the material, expressed in Eq. (18). However, this expression only fits in case of ohmic materials, that is, those who present a linear variation of the current flow with applied voltage. In case of materials with a very semiconductive behavior, where the hopping conduction is the main transport mechanisms, the correlation between the applied voltage and the current passing through the materials follows an exponential law [46], which is typical for low-filled polymer composites, where the intrinsic and contact transport mechanisms are not so prevalent:

$$I = GV\exp(kV) \tag{22}$$

where G is the conductance at 0 V, and k is a fitting parameter indicating the exponential ratio between current and voltage. Here, a higher value of this parameter would denote a higher exponential correlation between I and V.

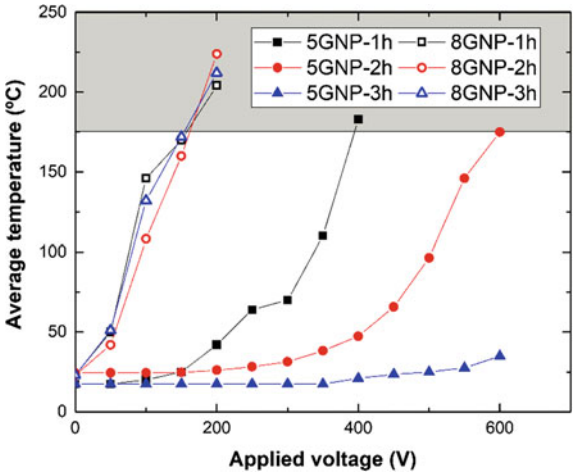

Fig. 17 Average temperature reached as a function of the applied voltage for a GNP-epoxy nanocomposites at different GNP contents and sonication time, where the gray-colored area indicates the degradation zone of the epoxy resin (reproduced from [11] under creative commons CC-BY license)

Therefore, in this case, the electrical conductivity at low voltage levels is much lower than at high voltage levels, and thus, the maximum temperature reached at high voltage levels would be much higher than expected by Joule's law.

On the other hand, in case of high-filled resins, the main transport mechanisms are due to intrinsic and contact effects between adjacent nanoparticles. Here, the *I*–*V* curve follows a linear fashion, and thus, they present an ohmic behavior. However, in this case, it has been elucidated that the electrical conductivity slightly decreases with temperature, so the maximum temperature reached as a function of voltage is lower than expected from the square law of Eq. (18). In this regard, Fig. 17 shows an example of temperature-voltage curves for Joule's heating test where the samples with the highest heating capabilities show a more linear response than those with the lowest heating response.

3 Applications of Electrically Conductive Polymers

Once understood the main electrical properties of conductive polymer matrices, it is important to explore the possible applications of this type of materials. In this regard, electrically conductive polymers open a wide range of applications in comparison with conventional polymers. Among these applications, their use as sensors, heaters, de-icing or self-healable systems is gaining a great deal of attention in the last decades.

3.1 Polymer-Based Strain and Damage Sensors

The use of nanofilled conductive polymers as strain and damage sensors is based on their electromechanical properties, which have been discussed previously.

Here, the main advantage of this type of sensors over the conventional metallic gauges is their high sensitivity. Whereas the gauge factor at low strains can reach 10–50 for GNP-based nanocomposites, in case of conventional metallic gauges is around 2–3. Therefore, the nanofilled resins can be used for the detection of very small strains.

In this regard, strain sensors may be divided in two broad groups: those for wearable devices, which require a huge flexibility and thus, very high failure strain; and those for structural applications, which require a high stiffness and strength.

3.1.1 Wearable Flexible Sensors

Most of thermosetting polymers are brittle, with high stiffness and very low failure strain. However, there are flexible thermosets, by working with systems with very low glass transition temperature. For example, one of the most used epoxy system for with high flexibility is based in poly(ethylene glycol) diglycidyl ether (PEGDGE) monomer, which presents a very low glass transition temperature (below room temperature), very high failure strain (up to 50%) and low stiffness; the ideal conditions for wearable devices.

Figure 18 shows an example of a CNT-PEGDGE system for the detection of small and large human movements. It can be observed that the high sensitivity of the system, due to the inherent piezoresistive behavior of the CNTs and the tunneling effect through the epoxy media, promotes a high motion detection.

Moreover, there are many research on wearable sensors based in nanofilled elastomers, such as polydimethylsiloxane (PDMS). Here, the electromechanical mechanisms are very similar to those commented before, but the elastomeric nature of the resin makes them highly applicable as wearable flexible devices.

Apart from the sensitivity for detection of large and small strain, the long-term stability is a crucial factor, as these sensors will be used in continuous cycling load conditions. In this context, it is important to study the electromechanical response when applying cycling load conditions. From Fig. 19, it can be observed that there is an initial decay of the electrical resistance. This can be associated to two effects: on the one hand, the inherent viscoelastic behavior of the elastomeric matrix, which promotes a delay between the electrical and the mechanical response and the possible irreversibility of the nanofiller network during the first stages of cycling load.

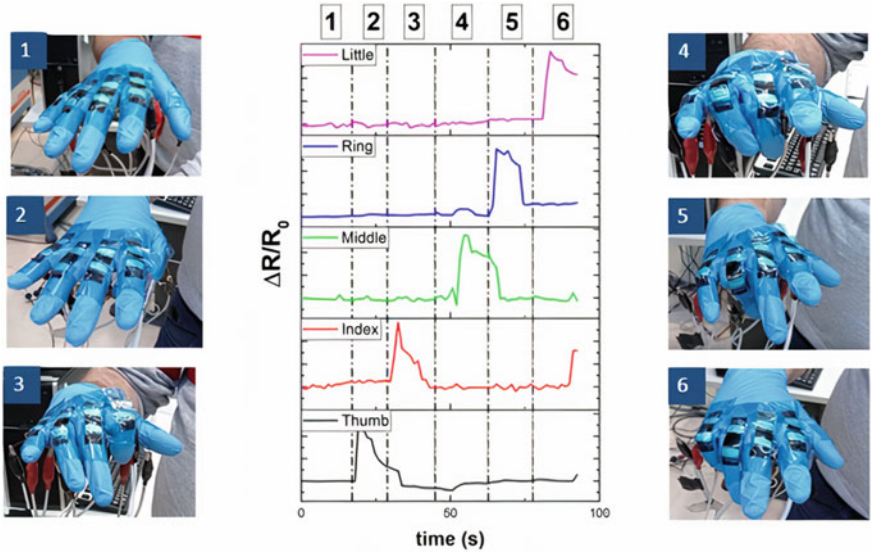

Fig. 18 Electromechanical measurements of finger motion monitoring in the case of fingers closing-opening for a CNT-PEGDGE wearable sensor (reproduced from [47] under creative commons CC-BY license)

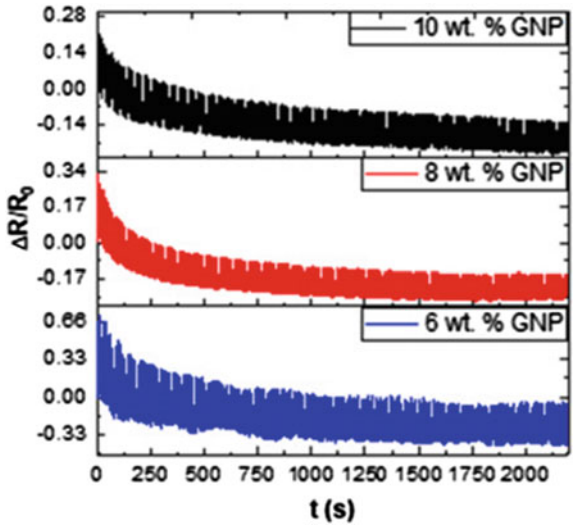

Fig. 19 Typical electromechanical response under cycling load in tensile conditions for a GNP-PDMS wearable system (reproduced with permission from [37])

3.1.2 Structural Electrically Conductive Polymers

The employment of structural conductive polymers for strain sensing and damage detection follows two main paths: their use as sensing coatings and their use as structural matrices in fiber-based multiscale composites.

In the first case, the development of electrically conductive polymers allows the creation of multifunctional smart coatings. In fact, there are many studies exploring their damage and strain sensing capabilities of nanofilled-based polymer coatings. It has been observed that, through electrical impedance tomography (EIT) techniques, which consists in the interpolation of electrical measurements through an electrode network, it is impossible to obtain an accurate mapping of the electrical conductivity of the material, making possible the identification of superficial defects [48].

In the second case, the use of nanofilled resins as matrices of fiber-based multiscale composites has been attracted the interest of many researchers. Here, it is possible to identify, not only the strain field throughout the material but also the presence of a wide range of defects such as matrix cracking, interfacial cracking or even, fiber breakage, as it induces a change in the surrounding strain field [49, 50]. In this regard, Fig. 20 shows an example of a multiscale CNT-GFRP composite under bending conditions. Here, it can be observed that it is possible to detect and locate the damage during the test, as the whole material acts as a sensor. This fact, in combination with their high sensitivity, makes nanofilled multiscale composites very promising materials for structural health monitoring (SHM) applications. The use of EIT techniques, as well as in case of polymer coatings, also offers a rapid mapping of defects in multiscale glass fiber composites [51, 52].

3.2 Applications as Electro-Thermal Heaters, De-Icing Devices, and Self-Healable Systems

The electro-thermal capabilities of nanofilled resins open a way for a wide range of applications including electro-thermal heaters for de-icing or self-healable devices.

Their capability as electro-thermal heaters is based on the extremely high efficiency of Joule's heating. More specifically, the heating rates that can be achieved are much superior to those achieved by other conventional heating (i.e., conventional oven or UV). Furthermore, the heating rate is increased with applied voltage, as the kinetic energy of the nanofillers is increased. In this regard, heating rates ranging from 0.18 to 2.89 °C/s for applied voltages ranging from 25 to 100 V, respectively, have been reported for CNT reinforced epoxy resins [54].

In this regard, these exceptional electro-thermal capabilities can be used for a wide range of applications. For example, there are many research taking advantage of Joule's heating capabilities for out-of-autoclave curing [55, 56]. Here, their fast heating rate in combination with a good nanofiller distribution is the crucial factors to ensure an homogeneous curing of the polymer matrix.

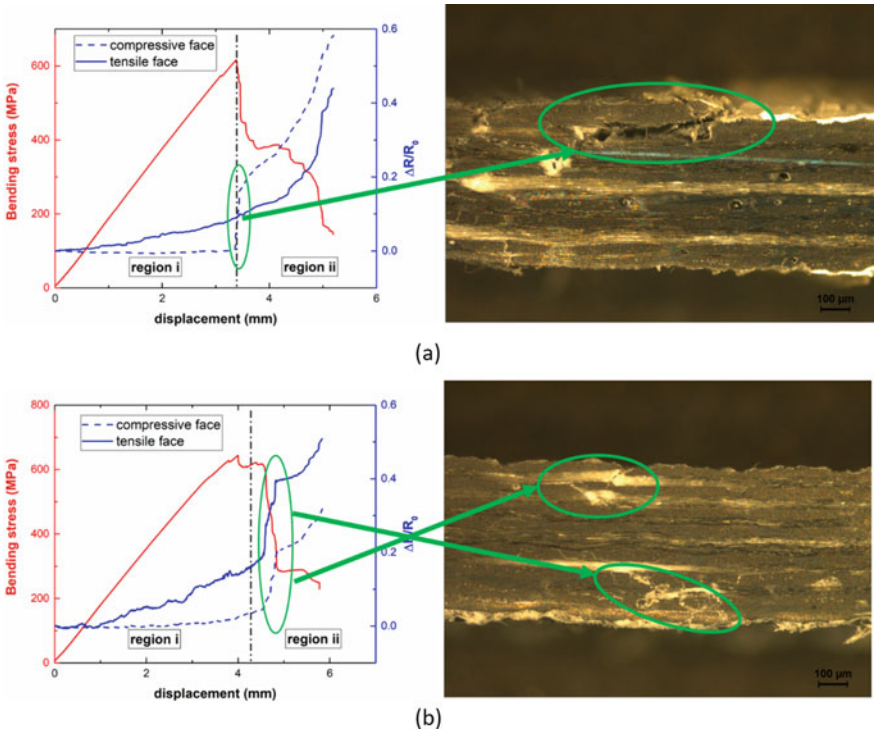

Fig. 20 Electromechanical response of glass fiber multiscale composites based on polycraplactone-epoxy blends filled with CNTs showing **a** a prevalent compressive failure and **b** mixed tensile-compressive failure, where the micrographs on the lefts denote the transversal sections (reproduced from [53] under creative commons CC-BY license)

Apart from curing by Joule's effect, this type of materials is commonly used for de-icing applications [57]. Here, when the ice is formed over the material surface, the application of an external voltage promotes an adequate surface heating, leading to the ice-melting. As observed in the graphs of Fig. 21, the de-icing capabilities of GNP-polymer composites are quite good, promoting an adequate, and fast ice-melting. Furthermore, most of the nanofillers enhance the hydrophobicity of the polymer matrix, avoiding the ice formation, as the wettability of water drops over these surfaces are quite poor.

Finally, another interesting application of the electro-thermal capabilities of nanofilled thermosetting resins is correlated to the development of self-healable systems. In this regard, self-healing refers to the capability of a material to restore their initial state after a damage takes place. Here, this self-healing capability can be achieved by an intrinsic or extrinsic stimulus. The external stimulus is usually based on healing processes that occurs by thermal activation. Therefore, heating by Joule's effect can be used to activate this external stimulus and promote the healing process inside the material.

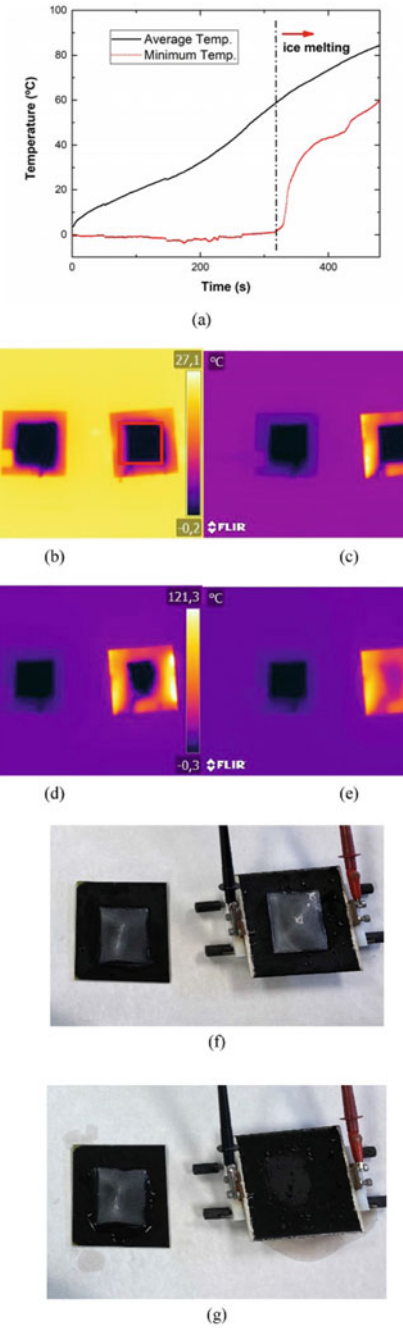

Fig. 21 **a** Temperature profile during de-icing tests of a GNP-epoxy coating, IR images at **b** initial state and after **c** 2 min, **d** 4 min, and **e** 6 min of voltage application and photographs showing **f** the initial state and **g** complete de-icing after Joule's heating test where the left specimen corresponds to the reference coating and the right one to the Joule's heated (reproduced from [60] under creative commons CC-BY license)

The self-healing process under Joule's heating is now gaining a great deal of attention. For example, some self-healable systems are comprised by blends of thermoplastic particles, such as polycaprolactone (PCL) and epoxy resins. Here, if the temperature reached is above the melting point of PCL, this thermoplastic phase may flow, filling a crack. The efficiency of self-healing process has proved to be very high, over 70% [58], indicating that the healing activation by Joule's heating is quite promising and avoids the use of conventional heating sources that are usually much less autonomous. Another example of self-healable systems activated by thermal stimulus is based on the presence of reversible bonds, such as Diels–Alder (DA) and retro-Diels–Alder (rDA) reactions. Here, the activation by Joule's effect has shown healing efficiencies of above 90% [59], proving the high potential of electro-thermal process for this type of self-healable systems.

4 Conclusions

Throughout this chapter, the electrical properties of polymers have been discussed. More specifically, the main transport mechanisms involving electrically conductive polymer composites have been discussed.

It has been observed that there are a wide range of conductive micro and nanofillers that can be incorporated to polymer resins: metal, carbon-based, ceramic, and metal-coated fillers. Here, the percolation threshold, that is, the critical volume fraction where the electrical pathways are created, promoting an electrically conductive network, is a critical parameter. It depends on the aspect ratio of the nanofillers, their dispersion state, and the possible interactions among them.

Furthermore, the main transport mechanisms were identified as intrinsic electrical conductivity of nanofillers, contact, and tunneling resistance between adjacent and neighboring nanoparticles. The first one depends on the nanofiller nature, whereas the contact and tunneling ones are influenced by the nanofiller, the insulating media, and the interactions nanofiller-polymer. More specifically, the interparticle distance, the tunneling area, and the height barrier of the insulating media were identified as the main parameters governing tunneling transport.

In addition, the linear-exponential correlation of tunneling resistance with interparticle distance makes nanofilled-based resins very susceptible to electrical changes with applied strain. Here, the sensitivity achieved in these systems is quite above that found in conventional strain gauges, making them very promising for strain sensing and damage detection devices.

Moreover, the electro-thermal properties of the nanofilled resins make them very susceptible to heating by Joule's effect, that is, by the application of an external electrical field. This interesting property can be used to develop thermo-electrical heaters, de-icing systems or to stimulate thermal activation of self-healing processes.

Therefore, it can be concluded that a good understanding of electrical properties of polymers is a key factor to take advantage of their multiple functionalities.

References

1. Senturia, S.D., Sheppard, N.F.: Dielectric analysis of thermoset cure. In: Epoxy Resins and Composites IV, pp. 1–47. Springer (1986)
2. Pitt, C., Barth, B., Godard, B.: Electrical properties of epoxy resins. IRE Trans. Compon. Parts. **4**, 110–113 (1957)
3. Aradhana, R., Mohanty, S., Nayak, S.K.: A review on epoxy-based electrically conductive adhesives. Int. J. Adhes. Adhes. **99**, 102596 (2020)
4. Yim, B., Kwon, Y., Oh, S.H., Kim, J., Shin, Y., Lee, S.H., Kim, J.: Characteristics of solderable electrically conductive adhesives (ECAs) for electronic packaging. Microelectron. Reliab. **52**, 1165–1173 (2012)
5. Ardanuy, M., Rodríguez-Perez, M.A., Algaba, I.: Electrical conductivity and mechanical properties of vapor-grown carbon nanofibers/trifunctional epoxy composites prepared by direct mixing. Compos. B Eng. **42**, 675–681 (2011)
6. Zhao, J., Hu, J., Jiao, D., Tosto, S.: Application of face centred cubic TiB powder as conductive filler for electrically conductive adhesives. Trans. Nonferrous Metals Soc. China. **24**, 1773–1778 (2014)
7. Tee, D.I., Mariatti, M., Azizan, A., See, C.H., Chong, K.F.: Effect of silane-based coupling agent on the properties of silver nanoparticles filled epoxy composites. Compos. Sci. Technol. **67**, 2584–2591 (2007)
8. Feng, Q., Yang, J., Fu, S., Mai, Y.: Synthesis of carbon nanotube/epoxy composite films with a high nanotube loading by a mixed-curing-agent assisted layer-by-layer method and their electrical conductivity. Carbon **48**, 2057–2062 (2010)
9. Sánchez-Romate, X.F., Artigas, J., Jiménez-Suárez, A., Sánchez, M., Güemes, A., Ureña, A.: Critical parameters of carbon nanotube reinforced composites for structural health monitoring applications: empirical results versus theoretical predictions. Compos. Sci. Technol. **171**, 44–53 (2019)
10. Bryning, M.B., Islam, M.F., Kikkawa, J.M., Yodh, A.G.: Very low conductivity threshold in bulk isotropic single-walled carbon nanotube–epoxy composites. Adv. Mater. **17**, 1186–1191 (2005)
11. Sánchez-Romate, X.F., Sans, A., Jiménez-Suárez, A., Campo, M., Ureña, A., Prolongo, S.G.: Highly multifunctional GNP/epoxy nanocomposites: from strain-sensing to joule heating applications. Nanomaterials. **10**, 2431 (2020)
12. Li, Y., Kanaji, N., Wang, X., Sato, T., Nakanishi, M., Kim, M., Michalski, J., Nelson, A.J., Farid, M., Basma, H., Patil, A., Toews, M.L., Liu, X., Rennard, S.I.: Prostaglandin E2 switches from a stimulator to an inhibitor of cell migration after epithelial-to-mesenchymal transition. Prostaglandins Other Lipid Mediat. **116–117**, 1–9 (2015)
13. Saad, G.R., Ezz, A.A., Ahmed, H.A.: Cure kinetics, thermal stability, and dielectric properties of epoxy/barium ferrite/polyaniline composites. Thermochim. Acta **599**, 84–94 (2015)
14. Martin-Gallego, M., López-Manchado, M.A., Calza, P., Roppolo, I., Sangermano, M.: Gold-functionalized graphene as conductive filler in UV-curable epoxy resin. J. Mater. Sci. **50**, 605–610 (2015)
15. Krushnamurty, K., Rini, M., Srikanth, I., Ghosal, P., Das, A.P., Deepa, M., Subrahmanyam, C.: Conducting polymer coated graphene oxide reinforced C–epoxy composites for enhanced electrical conduction. Compos. A Appl. Sci. Manuf. **80**, 237–243 (2016)
16. Moriche, R., Sanchez, M., Jimenez-Suarez, A., Prolongo, S.G., Urena, A.: Strain monitoring mechanisms of sensors based on the addition of graphene nanoplatelets into an epoxy matrix. Compos. Sci. Technol. **123**, 65–70 (2016)
17. Wu, K.H., Ting, T.H., Wang, G.P., Ho, W.D., Shih, C.C.: Effect of carbon black content on electrical and microwave absorbing properties of polyaniline/carbon black nanocomposites. Polym. Degrad. Stab. **93**, 483–488 (2008)
18. Sánchez-Romate, X.F., Jiménez-Suárez, A., Sánchez, M., Güemes, A., Ureña, A.: Novel approach to percolation threshold on electrical conductivity of carbon nanotube reinforced nanocomposites. Rsc Adv. **6**, 43418–43428 (2016)

19. Milowska, K., Birowska, M., Majewski, J.A.: Mechanical and electrical properties of carbon nanotubes and graphene layers functionalized with amines. Diam. Relat. Mater. **23**, 167–171 (2012)
20. Li, J., Ma, P.C., Chow, W.S., To, C.K., Tang, B.Z., Kim, J.: Correlations between percolation threshold, dispersion state, and aspect ratio of carbon nanotubes. Adv. Func. Mater. **17**, 3207–3215 (2007)
21. Kovacs, J.Z., Velagala, B.S., Schulte, K., Bauhofer, W.: Two percolation thresholds in carbon nanotube epoxy composites. Compos. Sci. Technol. **67**, 922–928 (2007)
22. Takeda, T., Shindo, Y., Kuronuma, Y., Narita, F.: Modeling and characterization of the electrical conductivity of carbon nanotube-based polymer composites. Polymer **52**, 3852–3856 (2011)
23. Kuronuma, Y., Takeda, T., Shindo, Y., Narita, F., Wei, Z.: Electrical resistance-based strain sensing in carbon nanotube/polymer composites under tension: analytical modeling and experiments. Compos. Sci. Technol. **72**, 1678–1682 (2012)
24. Sánchez, M., Moriche, R., Sánchez-Romate, X.F., Prolongo, S.G., Rams, J., Ureña, A.: Effect of graphene nanoplatelets thickness on strain sensitivity of nanocomposites: a deeper theoretical to experimental analysis. Compos. Sci. Technol. **181**, 107697 (2019)
25. Oskouyi, A.B., Sundararaj, U., Mertiny, P.: Tunneling conductivity and piezoresistivity of composites containing randomly dispersed conductive nano-platelets. Materials. **7**, 2501–2521 (2014)
26. Bao, W.S., Meguid, S.A., Zhu, Z.H., Meguid, M.J.: Modeling electrical conductivities of nanocomposites with aligned carbon nanotubes. Nanotechnology **22**, 485704 (2011)
27. Bao, W.S., Meguid, S.A., Zhu, Z.H., Pan, Y., Weng, G.J.: A novel approach to predict the electrical conductivity of multifunctional nanocomposites. Mech. Mater. **46**, 129–138 (2012)
28. Jangam, S., Raja, S., Maheswar Gowd, B.U.: Influence of multiwall carbon nanotube alignment on vibration damping of nanocomposites. J. Reinf. Plast. Compos. **35**, 617–627 (2016)
29. Moriche, R., Jiménez-Suárez, A., Sánchez, M., Prolongo, S.G., Ureña, A.: Sensitivity, influence of the strain rate and reversibility of GNPs based multiscale composite materials for high sensitive strain sensors. Compos. Sci. Technol
30. Sánchez-Romate, X.F., Moriche, R., Jiménez-Suárez, A., Sánchez, M., Prolongo, S.G., Ureña, A.: Sensitive response of GNP/epoxy coatings as strain sensors: analysis of tensile-compressive and reversible cyclic behavior. Smart Mater. Struct. **29**, 065012 (2020)
31. Zhai, T., Li, D., Fei, G., Xia, H.: Piezoresistive and compression resistance relaxation behavior of water blown carbon nanotube/polyurethane composite foam. Compos. A Appl. Sci. Manuf. **72**, 108–114 (2015)
32. Wichmann, M.H.G., Buschhorn, S.T., Boeger, L., Adelung, R., Schulte, K.: Direction sensitive bending sensors based on multi-wall carbon nanotube/epoxy nanocomposites. Nanotechnology **19**, 475503 (2008)
33. Moriche, R., Sanchez, M., Prolongo, S.G., Jimenez-Suarez, A., Urena, A.: Reversible phenomena and failure localization in self-monitoring GNP/epoxy nanocomposites. Compos. Struct. **136**, 101–105 (2016)
34. Sánchez-Romate, X.F., Jiménez-Suárez, A., Campo, M., Ureña, A., Prolongo, S.G.: Electrical properties and strain sensing mechanisms in hybrid graphene nanoplatelet/carbon nanotube nanocomposites. Sensors. **21**, 5530 (2021)
35. Tallman, T.N., Hassan, H.: A network-centric perspective on the microscale mechanisms of complex impedance in carbon nanofiber-modified epoxy. Compos. Sci. Technol. **181**, 107669 (2019)
36. Burke, P.J.: An RF circuit model for carbon nanotubes. IEEE Trans. Nanotechnol. **2**, 55–58 (2003)
37. Bosque, A.D., Sánchez-Romate, X.F., Sánchez, M., Ureña, A.: Ultrasensitive and highly stretchable sensors for human motion monitoring made of graphene reinforced polydimethylsiloxane: electromechanical and complex impedance sensing performance. Carbon. **192**, 234–248 (2022)
38. Cardoso, P., Silva, J., Agostinho Moreira, J., Klosterman, D., van Hattum, F.W.J., Simoes, R., Lanceros-Mendez, S.: Temperature dependence of the electrical conductivity of vapor grown

carbon nanofiber/epoxy composites with different filler dispersion levels. Phys. Lett. A. **376**, 3290–3294 (2012)
39. Beloborodov, I.S., Lopatin, A.V., Vinokur, V.M., Efetov, K.B.: Granular electronic systems. Rev. Mod. Phys. **79**, 469 (2007)
40. Bower, D.I.: No title. An Introduction to Polymer Physics (2003)
41. Jović, N., Dudić, D., Montone, A., Antisari, M.V., Mitrić, M., Djoković, V.: Temperature dependence of the electrical conductivity of epoxy/expanded graphite nanosheet composites. Scr. Mater. **58**, 846–849 (2008)
42. Weng, W., Chen, G., Wu, D.: Transport properties of electrically conducting nylon 6/foliated graphite nanocomposites. Polymer **46**, 6250–6257 (2005)
43. Kim, B., Park, S., Bandaru, P.R.: Anomalous decrease of the specific heat capacity at the electrical and thermal conductivity percolation threshold in nanocomposites. Appl. Phys. Lett. **105**, 253108 (2014)
44. Jeong, Y.G., An, J.: UV-cured epoxy/graphene nanocomposite films: preparation, structure and electric heating performance. Polym. Int. **63**, 1895–1901 (2014)
45. Sangroniz, L., Sangroniz, A., Fernández, M., Etxeberria, A., Müller, A.J., Santamaria, A.: Elaboration and characterization of conductive polymer nanocomposites with potential use as electrically driven membranes. Polymers **11**, 1180 (2019)
46. Pelech, I., Kaczmarek, A., Pelech, R.: Current-voltage characteristics of the composites based on epoxy resin and carbon nanotubes. J. Nanomaterials 405345 (2015)
47. del Bosque, A., Sánchez-Romate, X.F., Sánchez, M., Ureña, A.: Flexible wearable sensors based in carbon nanotubes reinforced poly (ethylene glycol) diglycidyl ether (PEGDGE): analysis of strain sensitivity and proof of concept. Chemosensors. **9**, 158 (2021)
48. Sánchez-Romate, XF., Moriche, R., Jiménez-Suárez, A., Sánchez, M., Prolongo, S.G., Güemes, A., Ureña, A.: Highly sensitive strain gauges with carbon nanotubes: from bulk nanocomposites to multifunctional coatings for damage sensing. Appl. Surf. Sci. **424**, 213–221 (2017)
49. Thostenson, E.T., Chou, T.: Carbon nanotube networks: sensing of distributed strain and damage for life prediction and self healing. Adv. Mater. **18**, 2837–+ (2006)
50. Gao, L., Chou, T., Thostenson, E.T., Zhang, Z., Coulaud, M.: In situ sensing of impact damage in epoxy/glass fiber composites using percolating carbon nanotube networks. Carbon **49**, 3382–3385 (2011)
51. Tallman, T.N., Gungor, S., Wang, K.W., Bakis, C.E.: Damage detection and conductivity evolution in carbon nanofiber epoxy via electrical impedance tomography. Smart Mater. Struct. **23**, 045034 (2014)
52. Tallman, T.N., Gungor, S., Wang, K.W., Bakis, C.E.: Damage detection via electrical impedance tomography in glass fiber/epoxy laminates with carbon black filler. Struct. Health Monit. **14**, 100–109 (2015)
53. Sánchez-Romate, X.F., Alvarado, A., Jiménez-Suárez, A., Prolongo, S.G.: Carbon nanotube reinforced poly (ε-caprolactone)/epoxy blends for superior mechanical and self-sensing performance in multiscale glass fiber composites. Polymers. **13**, 3159 (2021)
54. Donati, G., De Nicola, A., Munaò, G., Byshkin, M., Vertuccio, L., Guadagno, L., Le Goff, R., Milano, G.: Simulation of self-heating process on the nanoscale: a multiscale approach for molecular models of nanocomposite materials. Nanoscale Adv. **2**, 3164–3180 (2020)
55. Xia, T., Zeng, D., Li, Z., Young, R.J., Vallés, C., Kinloch, I.A.: Electrically conductive GNP/epoxy composites for out-of-autoclave thermoset curing through Joule heating. Compos. Sci. Technol. **164**, 304–312 (2018)
56. Sung, P., Chang, S.: The adhesive bonding with buckypaper–carbon nanotube/epoxy composite adhesives cured by Joule heating. Carbon **91**, 215–223 (2015)
57. Redondo, O., Prolongo, S.G., Campo, M., Sbarufatti, C., Giglio, M.: Anti-icing and de-icing coatings based Joule's heating of graphene nanoplatelets. Compos. Sci. Technol. **164**, 65–73 (2018)
58. Sánchez-Romate, X.F., Sans, A., Jiménez-Suárez, A., Prolongo, S.G.: The addition of graphene nanoplatelets into epoxy/polycaprolactone composites for autonomous self-healing activation by joule's heating effect. Compos. Sci. Technol. **213**, 108950 (2021)

59. Park, J.S., Kim, H.S., Thomas Hahn, H.: Healing behavior of a matrix crack on a carbon fiber/mendomer composite. Compos. Sci. Technol. **69**, 1082–1087 (2009)
60. Sánchez-Romate, X.F., Gutiérrez, R., Cortés, A., Jiménez-Suárez, A., Prolongo, S.G.: Multifunctional coatings based on GNP/epoxy systems: strain sensing mechanisms and joule's heating capabilities for deicing applications. Prog. Org. Coat. **167**, 106829 (2022)